Electronic Supplementary Material (ESI) for Energy Advances.

Electronic Supplementary Information:

Reversible Alkaline Hydrogen Evolution and Oxidation Reactions Using Ni–Mo Catalysts Supported on Carbon

Rituja B. Patil,[a] Manjodh Kaur, [a] Stephen D. House,[a,b] Lance Kavalsky,[d] Keda Hu,[e] Shirley Zhong,[f] Dilip Krishnamurthy,[d] Venkatasubramanian Viswanathan,[d] Judith Yang,[a,b,c] Yushan Yan,[e] Judith Lattimer,[f] and James R. McKone*[a]

[a]Department of Chemical and Petroleum Engineering, University of Pittsburgh, Pittsburgh, PA, 15260, USA
[b]Environmental TEM Catalysis Consortium (ECC), University of Pittsburgh, PA 15260, USA
[c]Dept. of Physics and Astronomy, University of Pittsburgh, PA 15260, USA
[d]Department of Mechanical Engineering, Carnegie Mellon University, Pittsburgh, PA, 15213, USA
[e]Versogen, Wilmington, DE, 19803, USA
[f]Giner, Newton, MA, 02466, USA
E-mail: jmckone@pitt.edu*, Phone: +1 (412)-384-7407

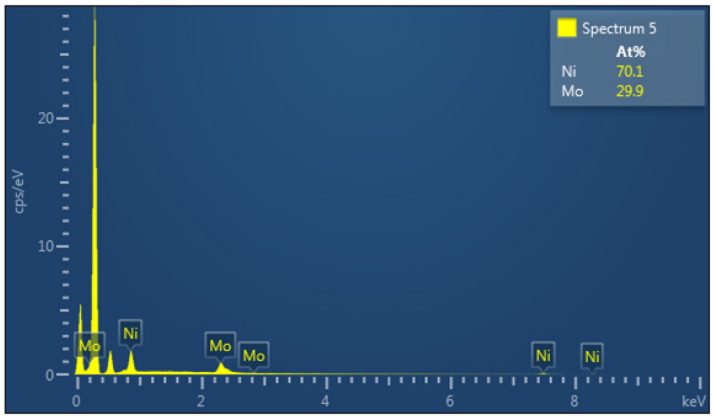

Figure S1. SEM-EDS analysis showing a 7:3 atomic ratio of Ni to Mo in the final reduced Ni–Mo/oC catalyst. This analysis reflects the aggregate composition of the sample on the micron scale, commensurate with the spot size of the electron beam.

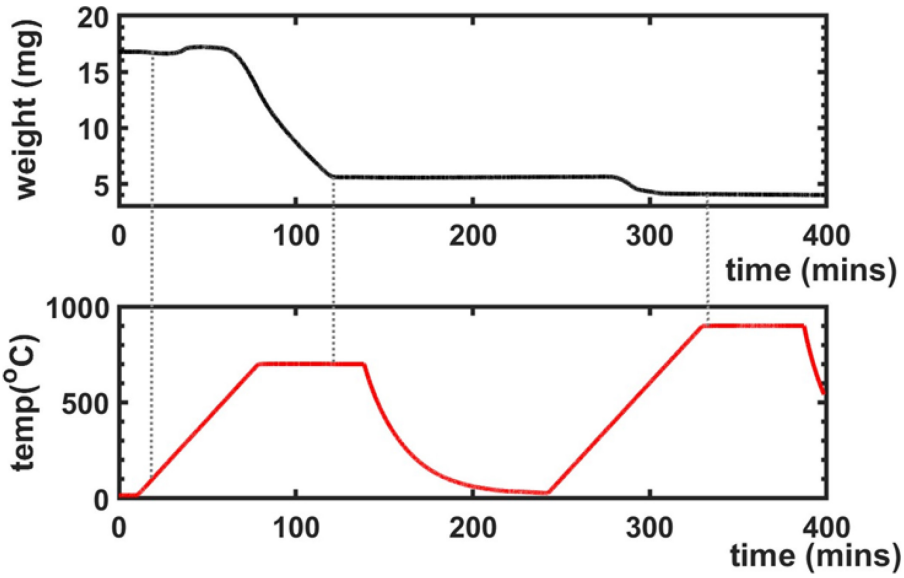

Figure S2. Representative thermogravimetric analysis (TGA) for 25 wt% Ni-Mo/oC showing mass change (black line) and sample temperature (red line) as a function of time. The

The TGA data in Figure S2 clearly show the weight loss for carbon content in the initial 100 min for the temperature increase to 700 °C under ambient air; this is likely coincident with complete oxidation of the Ni and Mo. The sample was then cooled to room temperature and heated again to 900 °C under reducing atmosphere, which leads to the reduction of metal oxide to metal. The total weight loss was 75 wt% of the initial amount, implying 25 wt% of the original sample was metal. Measurement uncertainty for the mass loading primary results from the possibility that some of the Mo remains oxidized even at 900 °C. Thus, the mass loadings reported herein are best interpreted as upper bounds, and the mass-normalized activities (e.g., current/mass) as lower bounds.

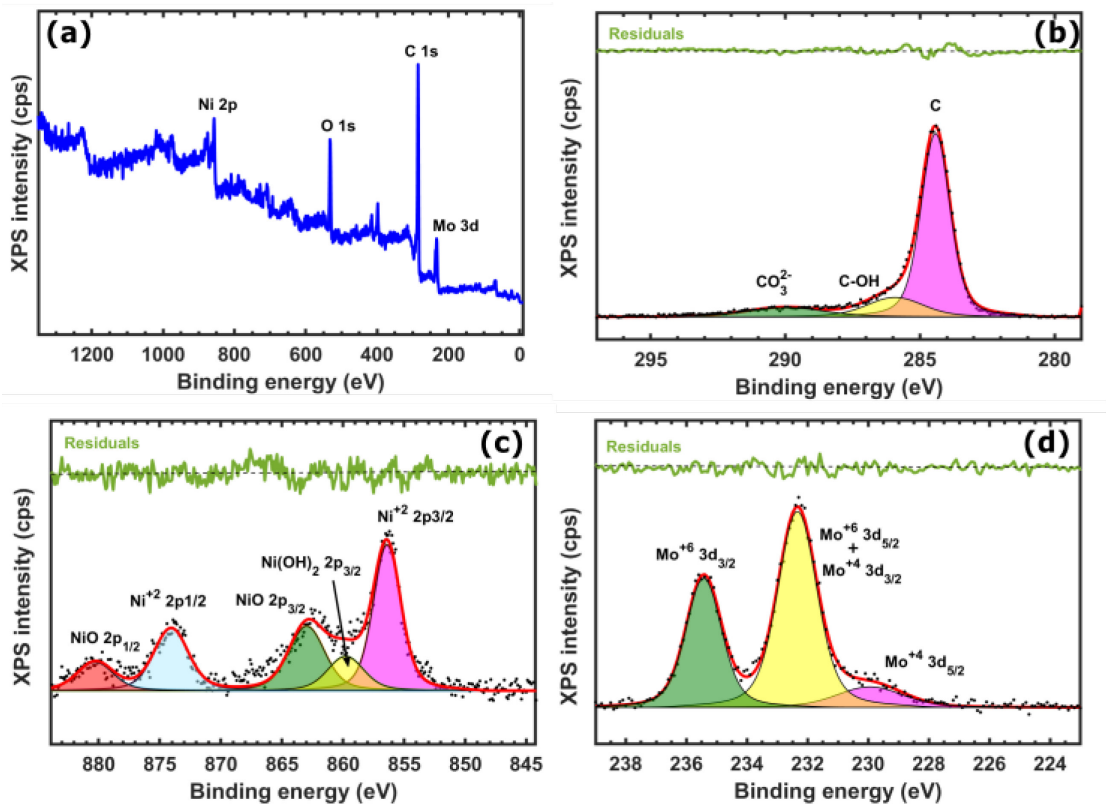

Figure S3. XPS data for 25 wt % Ni-Mo/oC: (a) survey scan indicating the presence of Ni, Mo, C, and O; deconvoluted peaks for (b) C 1s region (c) Ni 2p region; (d) Mo 3d region. Note that fits for Mo^{+6} $3d_{5/2}$ and Mo^{+4} $3d_{3/2}$ in panel (d) were lumped into a single feature because they exhibit nearly the same electron binding energy.

Figure S3a shows the XPS survey spectrum and confirms the presence of Mo, Ni, C, and O in the 25 wt% Ni-Mo/oC catalyst. The peaks for C 1s signal are much higher in intensity due to the high mass fraction of C in the sample. The deconvoluted peaks for the Ni 2p (Figure S3c) and Mo 3d (Figure S3d) regions show the predominant oxidation states are Ni^{2+} and Mo^{6+}. Considering the surface sensitivity of XPS, the presence of oxidized Ni and Mo on the surface of the catalyst is consistent with our understanding that the catalyst surface is prone to oxidation upon handling in air. We speculate that surface surface Ni hydroxides are likely to be reduced to metallic Ni under reducing conditions, but it the composition of the predominant active site(s) under reaction conditions remains to be determined.

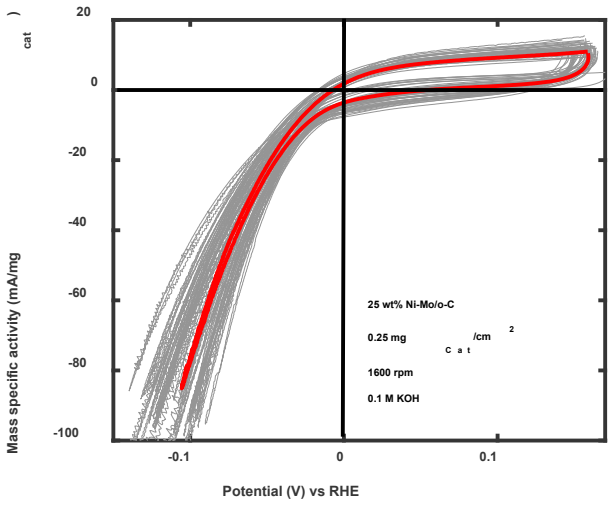

Figure S4. CV polarization curves for 25 wt% Ni-Mo/oC recorded at mass loading of 0.25 mg_{cat}/cm^2 for 50 different catalyst films at 1600 rpm. The electrolyte was H_2 saturated 0.1 M KOH(aq).

To illustrate uncertainty associated with activity measurements in this work, Figure S4 compiles CV data for each of 50 Ni–Mo/oC samples 0.25 mg_{cat}/cm^2 used for this study. The data highlighted in red in Figure S4 correspond to an empirical voltammogram whose mass specific cathodic current density at 100 mV HER overpotential (80 mA/mg) was nearly equal to the average of all 50 measurements.

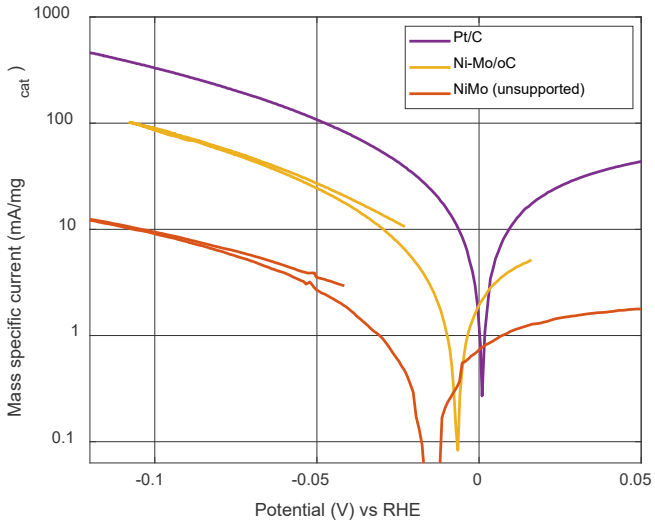

Figure S5. Tafel plot depiction of polarization data from main text Figure 3a comparing the mass specific activity of NiMo, NiMo/oC, and Pt/C. This depiction makes it easier to compare relative reaction rates at a fixed overpotential (e.g., -100 mV vs. RHE). Note that data for Ni were omitted because the cathodic current was negligible in this potential range.

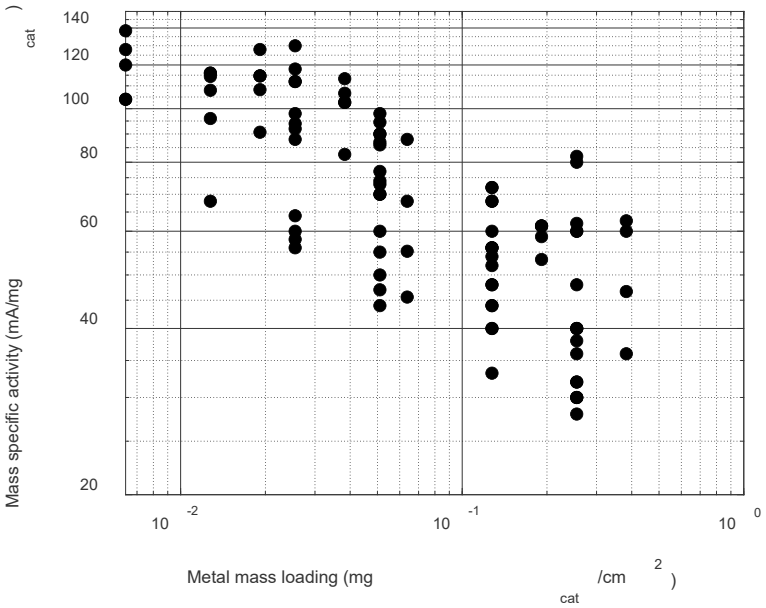

Figure S6. Current density at 100 mV HER overpotential as a function of metal mass loading for 25 wt% Ni–Mo/oC. Data were collected at 1600 rpm in H_2-saturated 0.1M KOH(aq). Note the lack of a clear asymptote to a single mass-specific activity even at <0.01 mg/cm^2, implying internal mass transfer limitations remain prevalent even at this low catalyst loading.

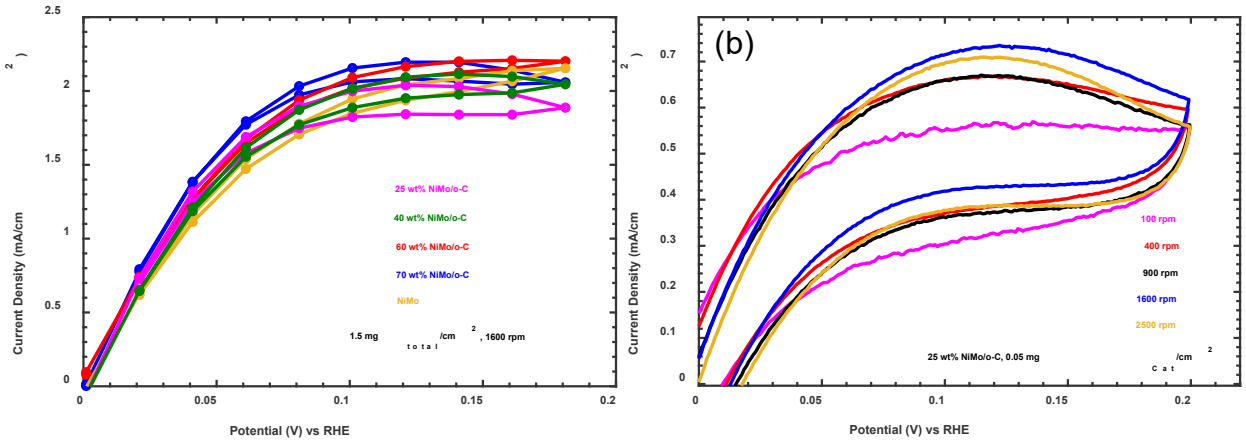

Figure S7. HOR polarization data for Ni–Mo/oC in 0.1 M KOH: (a) varying catalyst mass fraction while fixing the total catalyst loading on the electrode and the rotation rate; (b) varying rotation rate at a fixed catalyst mass fraction and mass loading.

Table S1. Compiled data for Ni-Mo-based catalysts for alkaline hydrogen evolution									
DOI Link	Catalyst Composition	Electrolyte	Mass loading (mg/cm^2)	Reported benchmark current density J (mA/cm2)	Overpotential η at benchmark J (mV)	J at η = 100 mV (mA/cm^2)	Mass activity at 10 mA/cm^2 (mA/mg)	Mass activity at η = 100 mV	Ref
http://dx.doi.org/10.1039/d1ee01487k	h-NiMoFe catalyst on a Ni foam	1M KOH	0.5	1000	97	1000	--	2000	[1]
http://dx.doi.org/10.1002/anie.202013047	Ni_4Mo alloy nanoparticles	0.1 M KOH	0.2	10	56	40	50.00	200	[2]
http://dx.doi.org/10.1016/j.electacta.2020.137151	N-doped carbon matrix with Ni_2P/MoP	1M KOH	0.07	10	78	13 (at $\eta \sim 90$mV)	140.85	183	[3]
10.1016/j.nanoen.2016.07.005	NiMo nanowires on Ni-foam	1M KOH	0.41	10	30	75	24.39	183	[4]
http://dx.doi.org/10.1021/acscatal.0c03355	($Ni_6Mo_6C/NiMoO_x$ on activated carbon cloth	1M KOH	0.6	10	29	50	16.67	83	[5]
This work	25 wt% NiMo/o-VC	0.1 M KOH	0.25	10	65	20	40.00	80	This work
10.1016/j.nanoen.2016.02.023	Ni-Mo-N nanocomposite	1M KOH	1	20	43	55	--	55	[6]
http://dx.doi.org/10.1002/adfm.202103673	Mo-Ni3N/Ni/NF	1M KOH	0.7	10	45	40	14	57	[7]
10.1002/smll.201701648	Ni–Mo nanosheets	1M KOH	0.8	10	35	45	12.5	57	[8]
https://doi.org/10.1016/0360-3199(82)90051-9	60:40 atomic ratio of Ni:Mo on mild steel mesh	5N KOH	12.3	100	60	600	--	49	[9]
10.1002/advs.201700644	1T-MoS2/Ni2+δOδ(OH)2-δ (1:1)	1M KOH	0.8	10	73	20	12.5	25	[10]
10.1021/cs300691m	Ni–Mo nano powder on Ti foil	2M KOH	1	20	70	20	--	20	[11]
http://dx.doi.org/10.1016/j.apcatb.2021.120494	P-doped Ni-Mo bimetal aerogel (Ni-Mo-P)	1 M KOH	1	10	69	15	10	15	[12]

Methodology & discussion of literature search for Table S1

An initial literature search was performed using the Clarivate Web of Science Database for publications between the beginning of 2013 and the end of 2022 with the following Boolean search criteria:

Keyword = {"Ni" OR "Nickel" or "nickel"} AND {"Mo" or "Molybdenum" or "molybdenum"} AND {"hydrogen evolution"}

This search returned approximately 2000 publications, predominantly including reports of catalysts containing both Ni and Mo along with several containing one or neither of these elements (which were excluded). These were further narrowed to ~400 based on the total number of citations: a cutoff of ≥20 citations per year was used for publications prior to 2020 and ≥20 citations total for publications appearing in 2020 and 2021; all publications that appeared in 2022 were included in the initial screen. Note that this methodology relies on the notion that reports of high-performing catalysts are likely to be more recent and more highly cited; to the extent this is not the case, our search may not have captured every relevant report.

The resulting set of ~400 publications were reviewed manually to extract two performance metrics that were most consistently reported: geometric current density at 100 mV overpotential and overpotential required to reach a geometric current density of 10 mA/cm^2. Table 1 was then constructed by down-selecting to publications reporting the best performance according to these metrics while excluding studies that did not report catalyst mass loading. Table S1 has been further organized in descending order of reported catalyst mass-activity (mA/mg) at 100 mV overpotential.

Notably, mass activity values for most of these reports fall in the range from 20–200 mA/mg at the benchmark overpotential of 100 mV. We speculate this is consistent with broadly similar HER active sites and mechanisms, despite differences in bulk composition and synthetic methods for each of these catalysts. Remaining differences within one order of magnitude may then be attributable to differences in active site density (which is a function of surface composition and specific surface area) and the extent to which experiments were carried out under conditions of kinetic vs. mixed kinetic-mass transfer control, as exemplified by the mass-loading dependence in Figure S6.

Cited References

1 Y. Luo, Z. Zhang, F. Yang, J. Li, Z. Liu, W. Ren, S. Zhang and B. Liu, *Energy Environ. Sci.*, 2021, **14**, 4610–4619.

2 M. Wang, H. Yang, J. Shi, Y. Chen, Y. Zhou, L. Wang, S. Di, X. Zhao, J. Zhong, T. Cheng, W. Zhou and Y. Li, *Angewandte Chemie International Edition*, 2021, **60**, 5771–5777.

3 Y. Xu, M. Yan, Z. Liu, J. Wang, Z. Zhai, B. Ren, X. Dong, J. Miao and Z. Liu, *Electrochimica Acta*, 2020, **363**, 137151.

4 M. Fang, W. Gao, G. Dong, Z. Xia, S. Yip, Y. Qin, Y. Qu and J. C. Ho, *Nano Energy*, 2016, **27**, 247–254.

5 X. Zheng, Y. Chen, X. Bao, S. Mao, R. Fan and Y. Wang, *ACS Catal.*, 2020, **10**, 11634–11642.

6 T. Wang, X. Wang, Y. Liu, J. Zheng and X. Li, *Nano Energy*, 2016, **22**, 111–119.

7 Y. Liu, J. Zhang, Y. Li, Q. Qian, Z. Li and G. Zhang, *Advanced Functional Materials*, 2021, **31**, 2103673.

8 Q. Zhang, P. Li, D. Zhou, Z. Chang, Y. Kuang and X. Sun, *Small*, 2017, **13**, 1701648.
9 D. E. Brown, M. N. Mahmood, A. K. Turner, S. M. Hall and P. O. Fogarty, *International Journal of Hydrogen Energy*, 1982, **7**, 405–410.
10 X. Zhang and Y. Liang, *Advanced Science*, 2018, **5**, 1700644.
11 J. R. McKone, B. F. Sadtler, C. A. Werlang, N. S. Lewis and H. B. Gray, *ACS Catal.*, 2013, **3**, 166–169.
12 B. Zhang, F. Yang, X. Liu, N. Wu, S. Che and Y. Li, *Applied Catalysis B: Environmental*, 2021, **298**, 120494.